

# FAST PROTON INDUCED PROCESSES ON NATURAL INDIUM

C. Oprea<sup>1,2,\*</sup>, A. Mihul<sup>2,3</sup>, I. Oprea<sup>1</sup>, S. Zgura<sup>4</sup>, M. Potlog<sup>4</sup>, A. Neagu<sup>4</sup>

<sup>1,\*</sup> *Joint Institute for Nuclear Research, Dubna (JINR), 141980 Russia*

<sup>2</sup> *Romanian Scientific Research Agency, Bucharest (ANCS), Romania*

<sup>3</sup> *European Center for Nuclear Research (CERN), 1211 Geneva 23, Switzerland*

<sup>4</sup> *Institute for Space Sciences, 077124 Magurele, Romania*

\*E-mail: coprea2005@yahoo.co.uk

Proton induced reactions with energies from threshold up to 25 MeV were investigated. Contributions of nuclear reaction mechanisms for each process are evaluated theoretically. For the protons up to 4–8 MeV, the compound processes are dominant and they are described by using a Hauser-Feshbach statistical approach. Contribution of direct mechanism to the cross section was determined using DWBA approach and pre-equilibrium processes by exciton model. At higher energies direct and pre-equilibrium mechanisms cannot be neglected. Parameters of optical potential and level density for incident and emergent channels were also extracted. The isotopes' production was analysed using cross sections calculated with Talys. Cross-section uncertainties provided by variation of optical potential parameters were also evaluated.

## INTRODUCTION

Nuclear reactions induced by fast charged particles (protons, alpha particles, deuterons, etc) are for a long time investigated at JINR Dubna basic facilities. These processes represent an efficient tool for fundamental researches of structure of atomic nuclei and nuclear reactions mechanism [1]. Reliable nuclear data of charged particle nuclear reactions are necessary as well for a large number of applications like neutron sources, proton therapy, isotopes production, transmutation and energy projects, accelerator physics and astrophysics [2–4].

In the present work  $^{113}\text{Sn}(p,2n)^{112}\text{Sn}$  and  $^{115}\text{In}(p,n)^{115}\text{Sn}$  nuclear reactions induced by fast neutrons with energies starting from threshold up to 25 MeV were investigated. Cross sections, Tin isotopes production and cross sections uncertainties were evaluated.

Indium is a chemical element with atomic  $Z = 49$  and two natural stable isotopes,  $^{113}\text{In}$  and  $^{115}\text{In}$ . Abundance of  $^{113,115}\text{In}$  nuclei are 4.29% and 95.71%, respectively. By interaction of Indium with fast protons followed by emission of gamma quanta and neutrons, Tin isotopes are obtained. This nucleus has a magic number of protons ( $Z = 50$ ) and therefore Tin has ten natural isotopes with atomic masses  $A = 112, 114, 115, 116, 117, 118, 119, 120, 122, 124$ , and abundances 0.96%, 0.66 %, 0.35 %, 14.30%, 7.61%, 24.03%, 8.58 %, 32.85%, 4.72 %, 5.94 %, respectively [5, 6].

## THEORETICAL BACKGROUND

Cross sections of  $^{113}\text{Sn}(p,2n)^{112}\text{Sn}$  and  $^{115}\text{In}(p,n)^{115}\text{Sn}$  reactions and Tin isotopes production in the fast protons were evaluated with Talys computer code.

Talys is a free software working under Linux dedicated to structure of atomic and nuclear reaction mechanisms calculations. In this code are implemented all nuclear reactions mechanisms, a nuclear database for a large number of stable nuclei and isotopes containing

spin, parity, energies, time of life of nuclear levels, parameters of density levels models and of Woods-Saxon potential with all components (volume, surface, spin-orbit, each with real and imaginary part) [7].

In Talys calculations all nuclear reaction mechanisms are enabled. Compound processes are described in the frame of Hauser-Feshbach approach [7, 8], exciton model is used for pre-equilibrium ones [7, 9], and Distorted Wave Born Approximation in the case of direct processes [7, 10].

Tin isotope production was modeled using cross section from Talys and charged particles energy loss in the target with finite given dimensions.

## RESULTS AND DISCUSSIONS

Cross sections, astrophysical rates, production of Tin isotopes and other were evaluated for  $^{113}\text{Sn}(p,2n)^{112}\text{Sn}$  and  $^{115}\text{In}(p,n)^{115}\text{Sn}$  processes with fast protons from threshold up to 25 MeV. For each reaction, contributions to the cross section of the nuclear reaction mechanisms and of the discrete and continuum states of residual nuclei were determined. Theoretical evaluations were compared with experimental data from literature. Production of Tin isotopes was modeled considering a target of natural Tin with transversal surface  $1\text{ cm}^2$ . Protons maximum energy was 35 MeV and in this case thickness is about 3 mm (protons remain in the target). Number of  $^{113}\text{In}$  nuclei is about  $5 \times 10^{20}$  and of  $^{115}\text{In}$  is  $1.1 \times 10^{22}$ . Irradiation time is 24 h and the protons intensity was chosen  $1\ \mu\text{A}$  and  $100\ \mu\text{A}$ , respectively.

*$^{113}\text{In}(p,2n)^{112}\text{Sn}$  reaction. Production of  $^{112}\text{Sn}$*

Tin isotope  $^{112}\text{Sn}$  was obtained in the  $^{113}\text{In}(p,2n)^{112}\text{Sn}$  reaction. Cross section energy dependence of  $^{113}\text{In}(p,2n)^{112}\text{Sn}$  process with fast protons starting from the threshold up to 25 MeV is represented in Fig. 1.

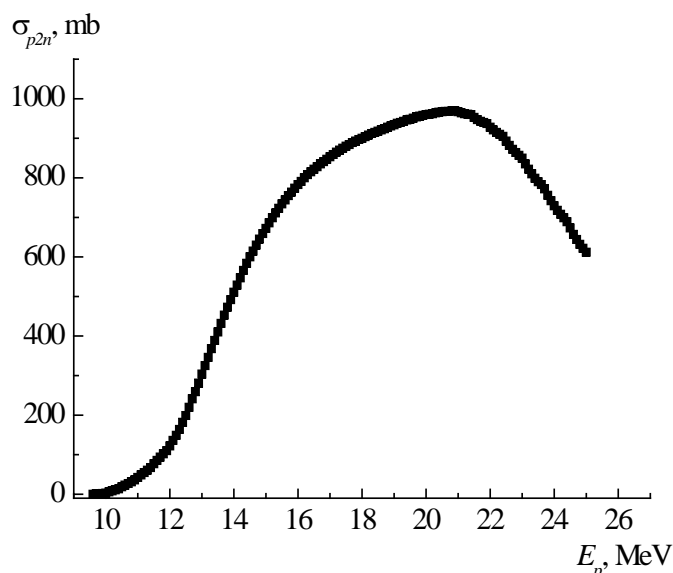


Fig. 1. Cross section of  $^{113}\text{In}(p,2n)^{112}\text{Sn}$  reaction.

Contributions to the cross section of the nuclear reaction mechanisms and of discrete and continuum states of the residual nucleus were determined. Talys evaluations showed that “pure” compound and multistep compound processes are dominant and the contribution of

other reaction mechanisms can be neglected for incident protons up to 25 MeV. Discrete states are important near the threshold ( $Q = -9.56$  MeV) and up to around 12 MeV. At higher proton energies, cross section is given mainly by continuum states.

Cross section of  $^{113}\text{In}(p,2n)^{112}\text{Sn}$  reaction has enough large values but there are no experimental data in the literature. Computer simulation of natural Tin interaction with 35 MeV protons for the  $^{112}\text{Sn}$  production given by  $^{113}\text{In}(p,2n)$  process contributes much greater than 1 ppm for 1  $\mu\text{A}$  and 100  $\mu\text{A}$  currents. Results are represented in Fig. 2.

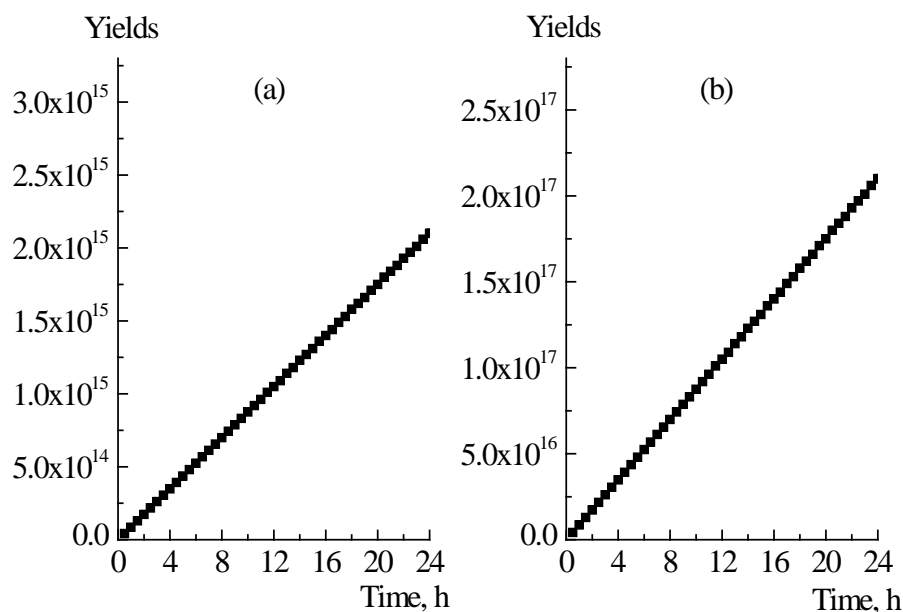


Fig. 2. Production of  $^{112}\text{Sn}$  in  $^{113}\text{In}(p,2n)$ . Current: a) – 1  $\mu\text{A}$ ; b) – 100  $\mu\text{A}$ .

#### $^{115}\text{In}(p,n)^{115}\text{Sn}$ reaction. Production of $^{115}\text{Sn}$

In the interaction of fast protons with natural In, the Tin isotope with mass number 115 can be formed in  $^{115}\text{In}(p,n)^{115}\text{Sn}$  reaction. Cross sections of  $^{115}\text{In}(p,n)^{115}\text{Sn}$  process with protons, starting from threshold up to 25 MeV are presented in Fig. 3.

In Fig. 3a contributions of nuclear reaction mechanisms to the cross section are represented. Compound processes are dominant in the whole interval of incident protons energy (curve 3). Direct processes (curve 1) have very low values. Pre-equilibrium mechanism has higher values than direct processes but much lower value than compound ones in 10–15 MeV region. Usually, in this range, at other nuclear reactions, contribution of the compound processes is replaced by the pre-equilibrium mechanism.

In Fig. 3b cross section of  $^{115}\text{In}(p,n)^{115}\text{Sn}$  reaction is represented as the sum corresponding to the discrete (curve 1) and continuum (curve 2) states of residual nucleus. Contribution of discrete states has very low values and practically the cross section of  $(p,n)$  process (curve 3) coincides with the cross section given by continuum states (curve 2). Curve 4 from Fig. 3a is practically the same with curve 3 from Fig. 3b.

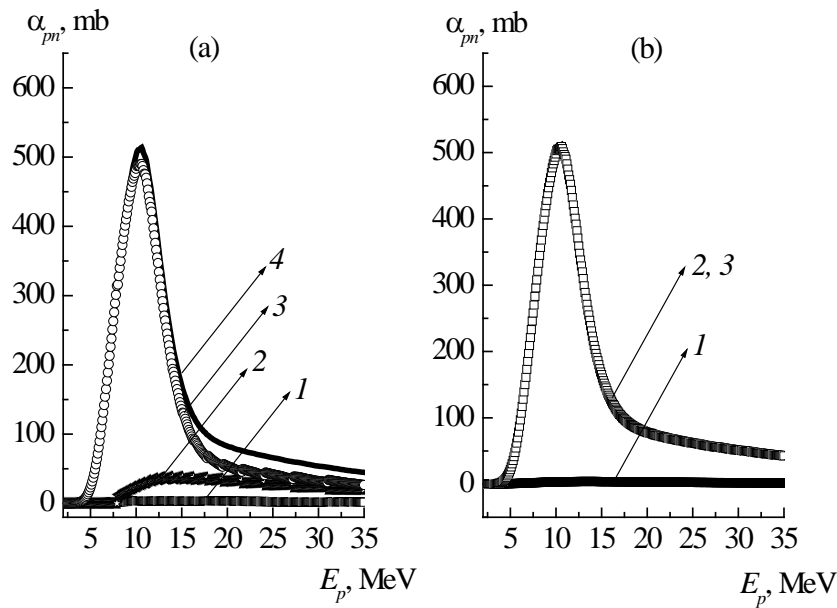


Fig. 3. Cross section of  $^{115}\text{In}(p,n)^{115}\text{Sn}$ . Mechanisms : a) 1 – direct; 2- pre-equilibrium; 3 – compound; 4 – sum of 1, 2, 3. States: b) 1 –discrete; 2 – continuum; 3 – sum of 1, 2.

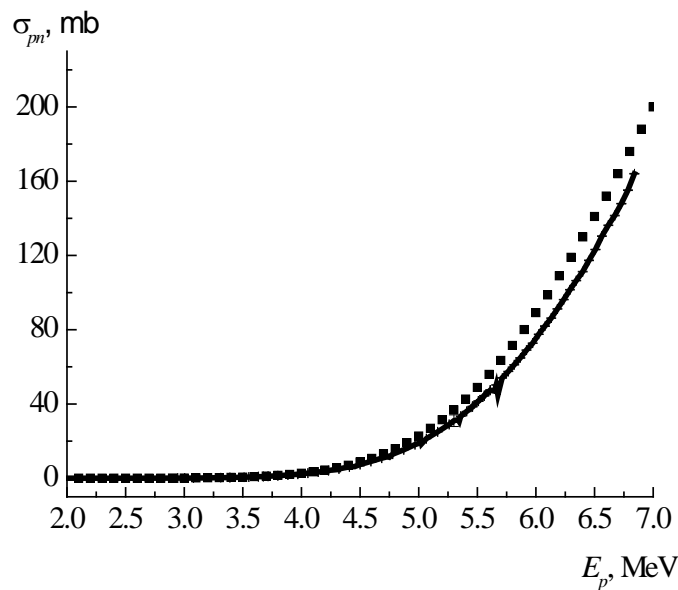


Fig. 4.  $^{115}\text{In}(p,n)^{115}\text{Sn}$ . Talys evaluation – line. Experimental data – points.

In Fig. 4 the theoretical evaluations are compared with experimental data. The good agreement between theory and experiment was obtained mainly by variation of the parameters of optical potential. Experimental data are from [11].

Like for other two processes analyzed before, the production of  $^{115}\text{Sn}$  in  $^{115}\text{In}(p,n)$  processes by interaction of 35 MeV fast protons on a natural Indium target were determined for 1  $\mu\text{A}$  and 100  $\mu\text{A}$  currents. Results are shown in the Fig. 5.

Production of  $^{115}\text{Sn}$  is higher than that of  $^{112}\text{Sn}$  isotopes for both proton currents. Tin isotope with mass number 115 is obtained from  $^{115}\text{In}$  which has a much larger abundance in

natural Indium in comparison with  $^{113}\text{In}$ , the source of  $^{112, 114}\text{Sn}$ , even when the cross section is larger.

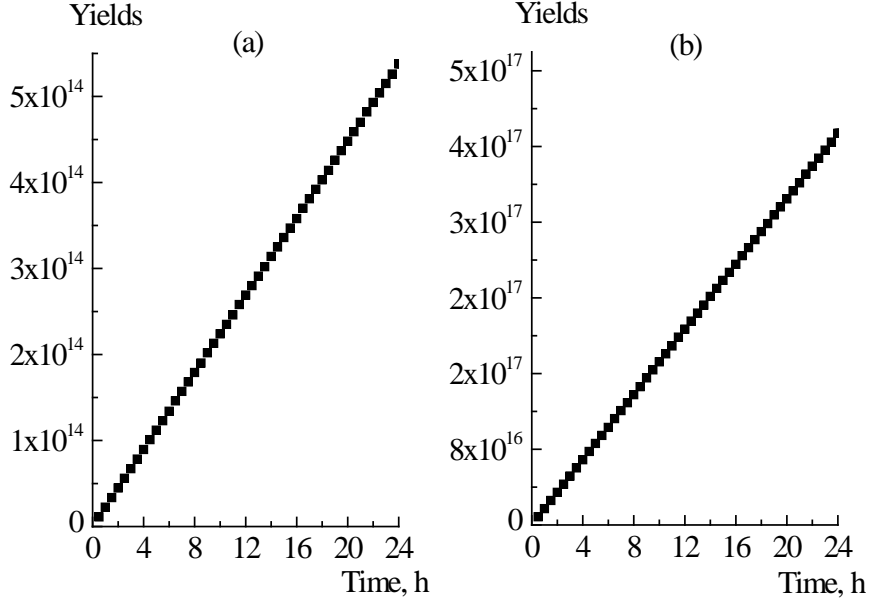


Fig. 5. Production of  $^{115}\text{Sn}$  in  $^{115}\text{In}(p,n)^{115}\text{Sn}$ . Current: a) 1 -  $\mu\text{A}$ ; b - 100  $\mu\text{A}$ .

#### *Parameters of optical potential*

Results presented in previous paragraphs were obtained with Talys using a large number of input parameters. In the cross section calculations were considered all open channels at the given incident energy. For elastic and inelastic channels, 30 levels of residual nucleus were taken into account and for reaction channels 10 levels. If the excitation energy is higher than excited states are considered in continuum [7]. Further, in this case, back - shifted Fermi gas model was chosen. The agreement between our evaluations and cross section data from literature was obtained by variation of optical potential parameters in the incident and emergent channels. In the calculations is used optical potential, with volume (V), surface (D) and spin-orbit (SO) components. Expression of Woods-Saxon potential (by components) is [7]:

$$U_{WS}(r) = V_V f(r, R_V, a_V) + iW_V f(r, R_W, a_W) - i4a_D W_D \frac{d}{dr} f(r, R_D, a_D) + V_{SO} \left( \frac{\hbar}{m_\pi c} \right)^2 \frac{1}{r} \frac{d}{dr} f(r, R_{VSO}, a_{VSO}) + iW_{SO} \left( \frac{\hbar}{m_\pi c} \right)^2 \frac{1}{r} \frac{d}{dr} f(r, R_{VSO}, a_{VSO}) \quad (1)$$

with the Wood-Saxon factor,  $f$ :

$$f(r, a_i, R_i) = \frac{1}{1 + \exp \frac{r - R_i}{a_i}} \quad \text{and} \quad R_i = R_{0i} A^{1/3} \quad (2)$$

where  $i$  represents the components  $V, D, SO$ ;  $A$  is the atomic mass;  $R_i$  is the radius;  $R_{0i}$  is the radius parameter;  $m_\pi$  is the pion mass;  $c$  is the speed of light.

Results with parameters of Woods-Saxon optical potential are presented in Table 1.

Process	$V_V$	$W_V$	$W_d$	$V_{SO}$	$W_{SO}$
$p + {}^{113}\text{In}$	62.42	0.11	4.25	6.09	-0.01
$p + {}^{115}\text{In}$	62.69	0.11	4.28	6.09	-0.01
$n + {}^{115}\text{Sn}$	50.74	0.14	3.94	6.09	-0.01

Table 1. Parameters of optical potential (in MeV) according with relation (3).

### Analysis of Uncertainties

Cross sections for  ${}^{113}\text{In}(p,2n){}^{112}\text{Sn}$  and  ${}^{115}\text{In}(p,n){}^{115}\text{Sn}$  reactions were evaluated. For their uncertainties analysis, parameters of optical potential from Table 1 for neutron and proton channels were modified starting with the half of initial value up to two times of the initial value. Evaluations showed that the cross sections are most sensible to the variation of the real part of the volume Woods-Saxon potential. In the Fig. 6 are represented the results for relative variation of the real and imaginary part of the volume Wood – Saxon potential, for proton incident channel, for  ${}^{115}\text{In}(p,n){}^{115}\text{Sn}$  reaction. In Fig. 5 the  $R$  ratios are defined as:

$$R(k, V_V) = \frac{\sigma_{p\gamma}(kV_V)}{\sigma_{p\gamma}(V_V)} \quad \text{and} \quad R(k, W_V) = \frac{\sigma_{p\gamma}(kW_V)}{\sigma_{p\gamma}(W_V)} \quad (3)$$

where  $k = 0.25, 0.5, 0.75, 1, 1.25, 1.5, 1.75, 2$ ;  $V_V, W_V$  are the real and imaginary part of volume Woods-Saxon potential with values from Table 1 ( $k=1$ );  $\sigma_{p\gamma}(V_V) = \sigma_{p\gamma}(W_V)$  are the  ${}^{113}\text{In}(p,\gamma){}^{114}\text{Sn}$  cross section (see Fig. 1a curve 4).

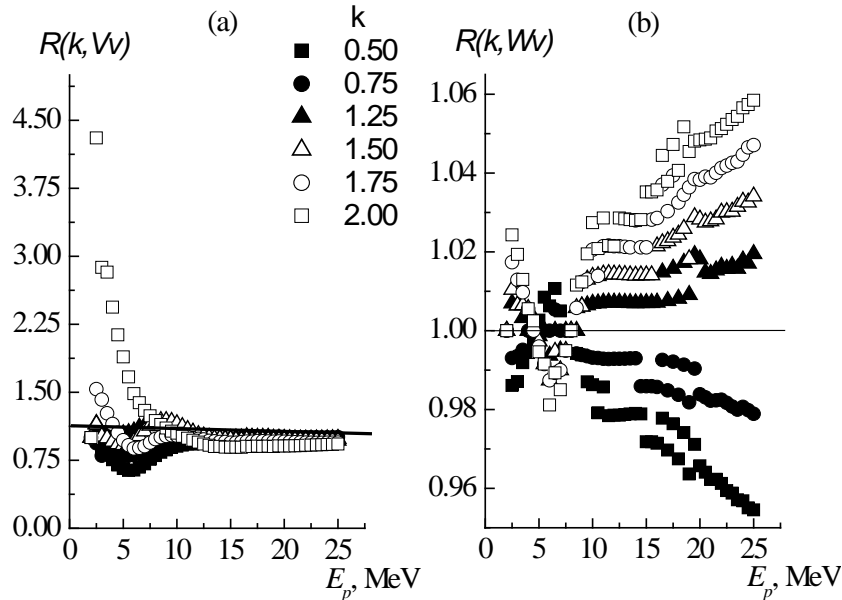


Fig. 6. The relative variation of the  ${}^{115}\text{In}(p,n){}^{115}\text{Sn}$  cross section by modifying the volume Woods-Saxon potential: a) real part; b) imaginary part. Line in both a) and b) represents the case  $k = 1$ .

Variation of the real part of the volume Woods-Saxon potential (given by  $k$  parameter) in the incident proton channel leads to the increasing of the cross section by four times near the threshold (Fig. 6.a). It is necessary to take into account the fact that near the threshold cross section has small values and the calculations can be affected by the computer codes precision here. Cross sections are influenced by the variation of the real part of volume Woods-Saxon potential starting from the threshold up to 10 MeV. This trend is maintained to other investigated processes from this work. Modification of the imaginary part of Woods-Saxon potential in the incident proton channel shows much lower changing in the cross sections (Fig. 6.b). As a general tendency, in the many investigated nuclear reactions, cross sections are the most sensitive to the modification of the real part of the volume Woods-Saxon potential in the incident and emergent channels, near the threshold up to 10–15 MeV.

## CONCLUSIONS

Interaction of fast protons with natural Indium and production of Tin isotopes for nuclear astrophysics were investigated. Cross sections of  $^{113}\text{In}(p,2n)^{112}\text{Sn}$  and  $^{115}\text{In}(p,n)^{115}\text{Sn}$  processes, for protons, from threshold up to 25 MeV were evaluated using Talys. Contribution of the nuclear reaction mechanisms related to the discrete and continuum states of residual nuclei were obtained. A good agreement between theoretical calculation and experimental data from literature was obtained. Optical potential parameters, for incident and emergent channels were also extracted.

Production of Tin isotopes was simulated for the analyzed processes in the case of a real finite dimensions target and different proton currents. Obtained results in computer simulation showed that the concentrations of Tin isotopes depend on the cross section and abundance of nuclei in the target. For chosen initial conditions, some of Tin isotopes can be measured in the activation experiments.

Many nuclear investigations and applications necessitate precise nuclear data. For this reason cross section uncertainties, related to the variation of optical potential parameters were analyzed. Results have demonstrated that the cross sections data are mainly influenced by the modification of the real part of the volume component of Wood – Saxon potential near the threshold and few MeV higher.

Present evaluations accomplished the necessity of new experimental and theoretical evaluations of protons induced processes as well as computer modeling for nuclear structure, reaction mechanisms and other investigations correlated with uncertainties studies of the resulted nuclear data.

***Acknowledgment.** The present researches are supported by JINR Dubna Annual Cooperation Program with Romanian Research Institutes coordinated by Romanian Plenipotentiary Representative and FLNP JINR Scientific Plan on 2021.*

## REFERENCES

- [1] A. Olacel, C. Borcea, M. Boromiza, Ph. Dessagne, G. Henning, M. Kerveno, L. Leal, A. Negret, M. Nyman, A.J.M. Plompen, *The European Physics Journal A*, Vol. **54**, p. 183 (2018).
- [2] S. Cabral, G. Borker, H. Klein, W. Mannhart, *Nucl. Sci. Eng.*, Vol. **106**, p. 308, (1990).
- [3] M. Salvatores, I. Slessarev, A. Tchistiakov, *Nucl. Sci. Eng.*, Vol. **130**, p. 309 (1998).

- [4] I. Gheorghe, D. Filipescu, T. Glodariu, D. Bucurescu, I. Cata-Danil, G. Cata-Danil, D. Deleanu, D. Ghita, M. Ivascu, R. Lica, N. Margineanu, R. Margineanu, C. Mihai, A. Negret, T. Sava, L. Stroe, S. Toma, O. Sima, M. Sin, *Nuclear Data Sheets*, Vol. **119**, p. 245 (2014).
- [5] J. Meija, T.B. Coplen, M. Berglund, W.A. Brand, P. De Bièvre, M. Groning, N.E. Holden, J. Irrgeher, R.D. Loss, T. Walczyk, T. Prohaska, *Atomic Weights of Elements* (IUPAC Technical Reports) , *Pure Appl. Chem.*, 2016, Vol. **88** no. 3, p. 265 (2013).
- [6] G. Audi, H.A. Wapstra, *Nucl. Phys. A*, Vol. **595**, p. 409 (1995).
- [7] A.J. Koning, S. Hilaire, M.C. Duijvestijn, TALYS-1.0., *Proceedings of the International Conference on Nuclear Data for Science and Technology*, April 22-27, 2007, Nice, France, editors O. Bersillon, F. Gunsing, E. Bauge, R. Jacqmin, S. Leray, EDP Sciences p. 211.(2008).
- [8] W. Hauser, H. Feshbach, *Phys. Rev.*, Vol. **87**, no. 2, p. 366 (1952).
- [9] A.J. Koning, M.C. Duijvestijn, *Nucl. Phys. A*, 2004, Vol. **744**, p. 15 (2004).
- [9] G.R. Satchler, *Direct Nuclear Reactions*, Oxford University Press: New York (1983).
- [10] S. Harissopulos, A. Spyrou, V. Fonteinou, M. Axiotis, G. Provas, P. Demetriou, *Phys. Rev. C*, Vol. **93**, p. 025804 (2016).
- [11] R.L. Hershberger, D.S. Flynn, F. Gabbard, P.H. Johnson, *Phys. Rev. C*, Vol. **21**, p. 896 (1980).